

Suitability of Recycled Polyethylene/Palm Kernel Shell-Iron Filings Composite for Automobile Application

I.A. Samotu^a, M. Dauda^a, F.O. Anafi^a, D.O. Obada^a

^aDepartment of Mechanical Engineering, Ahmadu Bello University, Zaria, Nigeria.

Keywords:

Composite
Palm-kernel
Shell
Ash
Particulate
Properties
Automobile
Bumper

ABSTRACT

A recycling aimed research was carried out to produce a new composite material and proffer suggestion for the possible use of the newly developed composite material. The empty water sachet (commonly called pure water nylon in Nigeria), was used as a matrix, which was reinforced by carbonized palm kernel shell (CPKS) particulate and iron fillings. The percentage composition of iron fillings was maintained at 5 wt%, while that of palm kernel shell ash was varied from 5 wt% - 20 wt% at an interval of 5 %. The composites were compounded and compressively moulded. Physical and mechanical properties of the composites were tested for alongside three conventional car bumper samples, and the results obtained shows that the composite material could be used to produce a car bumper among other parts of automobile like dashboard due to their impact strength and low density. Impact strength - density ratio for the materials gave prime information on the possible application of the developed material. Scanning Electron Microscope (SEM) was used to examine the distribution of the reinforcement within the matrix. After results analysis, materials with 5 wt% of CPKS and that with 10 wt% of CPKS were recommended for the car bumper production following their high impact strength - density ratio of 0.26 and 0.19 respectively, which are higher as compared to that of a conventional bumper material measured alongside the composite materials.

Corresponding author:

Ibraheem A. Samotu
Department of Mechanical
Engineering,
Ahmadu Bello University,
Zaria, Nigeria.
E-mail: omoobaawoo@gmail.com

© 2015 Published by Faculty of Engineering

1. INTRODUCTION

Empty water sachet (commonly called pure water nylon), Palm Kernel Shell and Iron Filings are waste all released into the environment from different sectors of production. These wastes, especially the empty water sachet, pose big challenges on the effort of achieving a clean and

safe environment, mostly by their contribution to flooding during the raining season.

The earliest racing cars were made mostly with a single aluminium chassis, which was prone to major fractures. In the late 1980s, the use of advanced composite material in the racing industry caused a revolution in the world of

automobile engineering. Such composites provided solution for racing car chassis, as these were not only lightweight, but also robust, offering the driver much more security, if the car were to crash [1].

The advantage of composite materials over normal single layered metals is the fact that these are many times stronger and lighter than the latter. As a result, the use of such a composite material not only decreases the overall weight of the object, but also, when compared to single layered materials, has more impact resistance [1].

According to Mangino and Indino [2], CO₂ emission from automobile through the use of composite material in their fabrication would be reduced from 167.5 g/km in 2003 then to 140 g/km in 2008 and it was expected to reduce further to 120 g/km by the year 2012.

In a developing country like Nigeria, where 80 % of the people are poor, according to World Bank report [3], sachet water cannot be easily substituted by table water for drinking purposes, as the table water cost more than five times that of sachet water. There is therefore the need to find ways of recycling the released empty water sachet into another useful material in view of its high consumption.

A lot of research has been carried out in the area of composite development. Use of palm kernel shell (PKS) based material for brake pad [4] some on automobile application [5,6] and many on suitability of some natural filler reinforced composite material [7-10]. Early research on the development and characterization of polymer/palm kernel Iron fillings composite has been reported [3] and by reason of the impact strength - density ratio for the materials, prime information on the possible application of the developed material was obtained.

Hence the objective of the present research is to study the suitability of a composite material, which is environmental friendly, recyclable, and made from renewable natural sources for parts fabrication in automobile. Hence this paper seeks to report the whole recyclability process including the comparative analysis.

Therefore, the specific objectives of this research are as follows:

- Development of new composite material from empty water sachet (recycled polyethylene), carbonized palm kernel shell and iron filings from our surroundings.
- Determination of the physical properties of the developed composite material.
- Determination of the mechanical properties of the developed composite material.
- Comparative analysis of the developed material to selected part of automobile to evaluate its suitability as a substitute material.

Finally, the major contribution of this research work is the recyclability of wastes in our environment for the production of another material of good properties, which can be used for diverse applications

2. MATERIALS AND METHODS

The materials used in this research were recycled low dense Polyethylene (RLDP), carbonized palm kernel shell (CPKS) and iron fillings.

2.1 Pre-Analysis on the Research Materials

Some pre-analyses were carried out on the research material before compounding them together to form the composite material. These were:

X-ray Fluorescence Test on CPKS

The test was carried out on an X-ray spectrometer, designed for elemental analysis of wide range of samples. The machine makes use of PW 4030 X-ray Spectrometer, which is an energy dispersion microprocessor controlled analytical instrument, designed for detection and measurement of elements in a sample, ranging from odium to uranium. The sample, being in powdery form was weighed and a binder (PVC dissolved in Toluene) was added to the sample, which was carefully mixed and pressed in hydraulic press into a pellet. The pellet was excited for a period of 15 minutes to generate the rays examined.

Tensile Test on Matrix Material

Tensile test was carried out on RLDP used as the matrix, before it was compounded with the reinforcement. The tensile properties were recorded for the material for comparison with the properties of the composite material.

2.2 Processing of the Composite Material

The percentage composition by weight of the RLDP and the carbonized palm kernel shell were varied while that of iron fillings was kept constant at 5 % as shown in Table 1.

Table 1. Formulation of Composite Material.

| S/n | Carbonized Palm Kernel | Iron Filings (wt%) | RLDP (wt%) | Sample Label |
|-----|------------------------|--------------------|------------|--------------|
| 1. | 0 | 0 | 100 | CPKS 0 |
| 2. | 5 | 5 | 90 | CPKS 5 |
| 3. | 10 | 5 | 85 | CPKS 10 |
| 4. | 15 | 5 | 80 | CPKS 15 |
| 5. | 20 | 5 | 75 | CPKS 20 |

The percentage of the iron filings was maintained at 5 wt% because earlier research shows that further addition of the filings will reduce the toughness of the composite [16].

Preparation of Recycled Polyethylene (RLDP)

Empty water sachets (made of polyethylene) were gathered from specific sources in Samaru community of Zaria, in Kaduna State of Nigeria. The sources were:

- A household of one occupant.
- A household of three occupants.
- A cafeteria on the campus of Ahmadu Bello University, Zaria, Nigeria.

These empty sachets were cut into small pieces for easy compounding and dried.

Preparation of Carbonized Palm Kernel Shell (CPKS)

Carbonized palm kernel shell was used for this research work. The fresh is raw shell obtained from palm oil processing firm. However, the ash was obtained from the fresh sample, using a technique called ‘ashing’, then, they were grinded and sieved.

Ashing

Palm kernel shells were heated in a furnace to 800 °C where they were turned into their carbon ash. This was done in order to retain their carbon content as fresh shell but with little moisture content. The Fig. 1 below shows sample of palm kernel ash obtained.



Fig. 1. Palm Kernel Ash Particulate.

Iron Filings Preparation

Iron filings were gathered from a grinding shop where mainly cast iron are being grinded, then sieved. Figure 2 below shows samples of iron filings gathered after sieving.



Fig. 2. Iron Filings gathered from Grinding Workshop.

Compounding

This is when all the materials were measured as specified for each composition then compounded together to form the composite.

After drying in an oven at 105 °C, the carbonized palm kernel shell particles, iron fillings and the polyethylene were compounded in a two roll mill at a temperature of 130 °C, into a homogenous mixture. 400 g of each composition were compounded and labelled. This was carried out at Nigerian Institute for Leather Science and Technology (NILEST), Samaru, Zaria, Nigeria.

Pressing

The composite after compounding were pressed to increase their compatibility. This was carried out on an electrically heated hydraulic press. The mixtures were placed in a square mould of length 150 mm and pressed with a pressure of 0.4 MN/m² until they cured. The temperature of both platens was maintained at 150 °C during the pressing. At the end of press cycle, boards were removed from the press for cooling then cut into specimens for characterization. All these processes go for all the four (4) compositions and the control. Figure 3 below shows sample of composite board obtained after pressing.



Fig. 3. Sample of the Board obtained after pressing.

2.3 Characterization of the Composite Material

Mechanical and Physical properties of the composite material were studied by carrying out the following tests on the material. Also samples of conventional car bumpers were obtained from bumpers of three prominent car models used in Nigeria, they were labelled Conventional Bumper Sample (CBS) 'A', 'B' and 'C'. Suitable specimen dimensioning and preparation were done to suit each test requirement according to standard.

Tensile Properties

Tensile strength indicates the ability of a composite material to withstand forces that pull it apart as well as the capability of the material to stretch prior to failure. Tensile tests were carried out using a Hounsfield Tensiometer, with maximum load of 250 KN. The standard specimens were mounted by their ends into the holding grips of the testing apparatus.

The machine is designed to elongate the specimen at a constant rate, and to measure the instantaneous applied load and the resulting elongations simultaneously using an extensometer. The ASTM standard test method for tensile properties of polymer composites with the designation D3039-76 was used (ASTM, 2000).

Hardness Test

The hardness test of composites is based on the relative resistance of its surface to indentation by an indenter of specified dimension under a specified load. Hardness of the composites were determined by using a direct reading Durometer, manufactured by Francisco Munoz Irlas, C.B. model: 5019 and Serial No: 01554. The Durometer measures the hardness of material according to ASTM D2240 ISO 7619. The Durometer measures in Shores. This was also done at NILEST.

Impact Energy Test

The impact tests of the composites sample were conducted using a fully instrumented Avery Denison test machine. Charpy impact tests were conducted on notched samples. Standard square impact test samples of dimensions 70 x 10 x 10 mm with notch depth of 2 mm and a notch tip radius of 0.02 mm at angle of 45° were used. The value of the angle through which the pendulum has swung before the test sample was broken corresponds with the value of the energy that will be absorbed in breaking the sample and this was read from the calibrated scale on the machine.

Density of PMCs

Densities of PMCs material were determined by simply using the relationship between volume and mass. A special technique for the determination of the density where pores are

taken into account is the determination by using water displacement (Archimedean density).

The basic method to determine the dry bulk density is using a specimen with regular shape (usually rectangular). By measuring the mass and with the knowledge of the volume, the density was calculated using the following expression [12]

$$\text{Density} = \frac{\text{Mass}}{\text{Volume}} \quad (1)$$

The density by the water displacement (Archimedean density) allows the determination of the density in air compared to its displacement in water or other liquid of known density. Depending upon the nature of the specimen (e.g., open or closed pore), the resultant value may deviate from the true mass.

2.4 Microstructural Analysis

Samples of the composite material were cut to dimension 10 mm X 10 mm X 5 mm. Samples after preparation were attached to multi-stub sample holder with the use of double sided conductive carbon tape, after which, they were mounted onto the specimen chamber, while the column was put at vacuum. After reaching the vacuum target, the electron gun was switch on which passed accelerating voltage of 20 kV and probe current of 227 pA through the samples at a working distance of 7.0 mm and/or 6.0 mm.

Micrographs of the composite material were taken in three magnifications along the span of the specimens. Scanning Electron microscope (SEM) EVO MA-10 manufactured by Carl, was used for the analysis at Sheda Science and Technology complex, Abuja, Nigeria.

3. RESULTS AND DISCUSSION

The results of analyses and tests carried out in the research are discussed below.

3.1 Pre-Analysis of the Research Materials

X-ray Fluorescence Test

The chemical composition of the carbonized palm kernel shell particulate as revealed by the test is summarized in the Table 2.

Table 2. Chemical Composition of the Palm Kernel Ash Particulate.

| Channel Compound | Percentage composition [%] |
|--------------------------------|----------------------------|
| Al ₂ O ₃ | 7.6 |
| SiO ₂ | 25.1 |
| P ₂ O ₅ | 2.4 |
| SO ₃ | 1.4 |
| K ₂ O | 15.0 |
| CaO | 12.3 |
| TiO ₂ | 0.92 |
| Cr ₂ O ₃ | 0.26 |
| MnO | 0.74 |
| Fe ₂ O ₃ | 12.3 |
| NiO | 0.2 |
| CuO | 1.4 |
| Yb ₂ O ₃ | 0.9 |

The results of the X-Ray Florescence test show that the carbonized palm kernel shell particulate possesses high percentage of silicon oxide which makes it suitable to be used as reinforcement but tends to give the composite material, some level of brittleness. It also accounts for its high refractoriness. Also, the results reveal high percentage composition of iron (Fe) and aluminium (Al), which accounts for the strength possessed by the ash after carbonizing.

Tensile Stress for the Matrix Materials

The load (N) and extension (mm) graph was obtained for the matrix (polyethylene) material while the tensile stress and strain were calculated. The tensile test carried out on the matrix material shows that the material has an ultimate tensile stress of 5.59 N/mm² but has high strain of 1554.80 %. These properties were compared with that of the composite material when measured to verify if the introduction of the reinforcement actually improves the properties of matrix.

3.2 PMCs Micrograph

Micrographs of the composite material, taken in three magnifications along the span of the specimens are presented in Figs. below. SEM was used to study the morphology of CPKS reinforced composites. Figures 4-6 show the SEM micrograph of the unreinforced polyethylene sample, while Figs. 7-9 show the SEM micrographs of the reinforced composites. Morphological analysis using SEM clearly show difference in the morphology of the unreinforced polyethylene sample and it composites (see Figs. 4-9). The microstructure clearly shows that when the CPKS particles were added to the unreinforced polyethylene sample, morphological change in the structure took place.

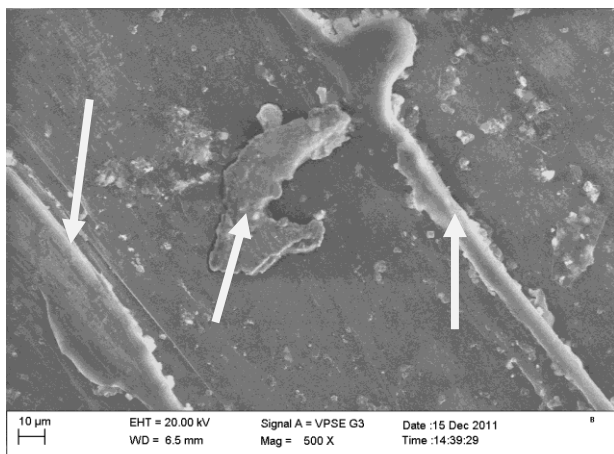


Fig. 4. Micrograph of Unreinforced RLDP (X500) showing chain of lamellae and inter lamella amorphous structure.

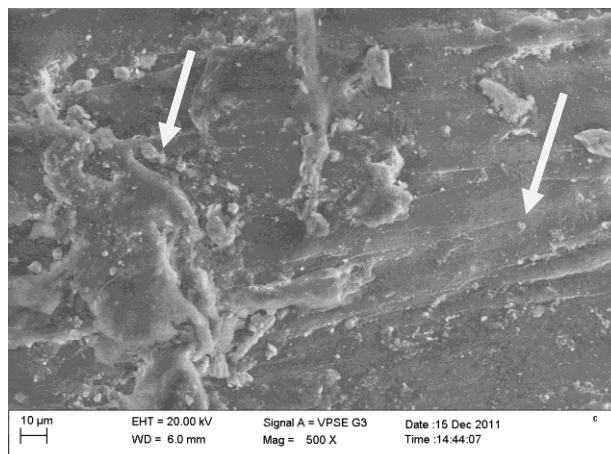


Fig. 7. Micrograph of Reinforced RLDP with 10% CPKS (X500) showing the presence of reinforcing particles grossly rejected by the polymer.

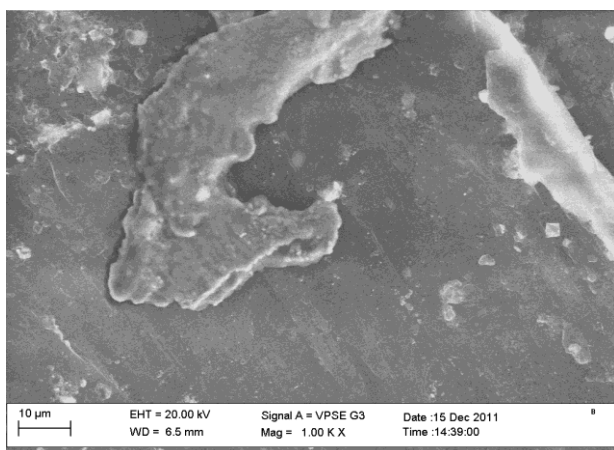


Fig. 5. Micrograph of Unreinforced RLDP (X1000) showing chain of lamellae and inter lamella amorphous structure.

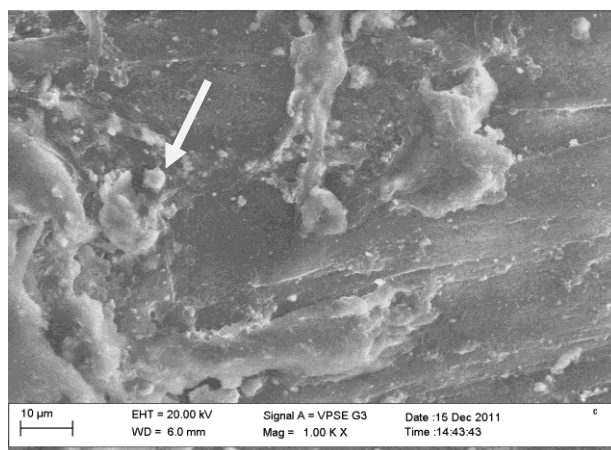


Fig. 8. Micrograph of Reinforced RLDP with 10% CPKS (X1000) showing the presence of reinforcing particles grossly rejected by the polymer.

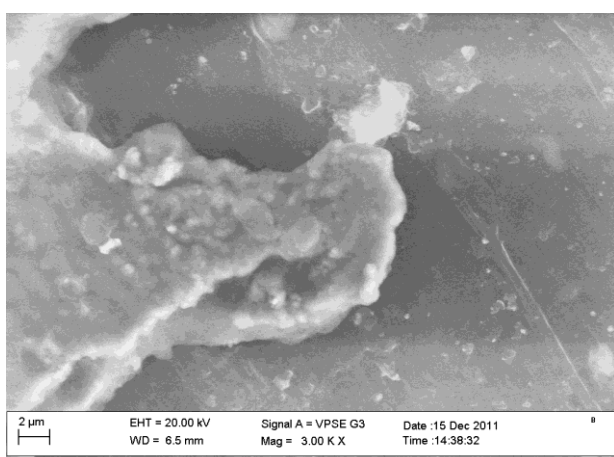


Fig. 6. Micrograph of Unreinforced RLDP (X3000) showing chain of lamellae and inter lamella amorphous structure.

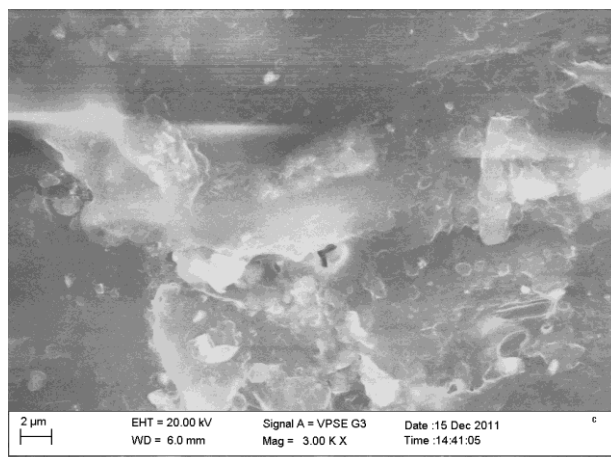


Fig. 9. Micrograph of Reinforced RLDP with 10% CPKS (X3000) showing the presence of reinforcing particles grossly rejected by the polymer.

The microstructure of the unreinforced polyethylene sample matrix reveals chain of lamellae and interlamella amorphous structure with linear boundaries between adjacent boundaries (Figs. 4-6). From the SEM micrograph, great pronouncement of the hydrophobic properties of the matrix leading to gross rejection of the reinforcements embedded in it was observed (Figs. 7-9). Due to the afore-mentioned effect, there was low inter-facial bonding between the reinforcements and the matrix. Particles-matrix interface plays an important role in composite properties. A strong particles-matrix interface bond is critical for high mechanical properties of composite [13]. This accounts for the low tensile strength possessed by the composite materials, which was decreasing with increase in the percentage composition of the reinforcement.

There was great variation in the sizes of the reinforcing particles, also uneven distribution of the reinforcing particles within the matrix was revealed by the micrograph. The relationship between the microstructure and the properties of the developed composite agrees with conclusions of other researchers [13-16].

3.3 Characterization of the Composite Material

Tensile Properties

The load (N) and extension (mm) graph was obtained for each composition, while the tensile stress and strain were calculated; The Ultimate Tensile Strength (U.T.S) and Breaking Stress were obtained from the graphs for each composition and recorded in Table 3.

Table 3. Tensile Properties of the Composite Material.

| Samples | Ultimate Tensile Strength (N/mm ²) | Breaking Stress (N/mm ²) | Tensile Modulus (N/mm ²) | Percentage Elongation (%) |
|---------|--|--------------------------------------|--------------------------------------|---------------------------|
| CPKS 0 | 8.24 | 7.50 | 25.55 | 87.29 |
| CPKS 5 | 7.94 | 5.75 | 24.08 | 79.45 |
| CPKS 10 | 7.37 | 6.41 | 24.46 | 45.54 |
| CPKS 15 | 6.90 | 5.34 | 29.92 | 41.85 |
| CPKS 20 | 4.43 | 2.73 | 19.20 | 37.50 |
| CBS A | 14.92 | 14.92 | 34.69 | 339.80 |
| CBS B | 10.08 | 8.98 | 29.67 | 109.82 |
| CBS C | 11.67 | 10.02 | 30.73 | 178.34 |

Figures below show the graphical representations of the Ultimate Tensile Strength, the Breaking Strength (B.S.), the Tensile

Modulus (ϵ) and Percentage Elongation (P.E.) for the composite material.

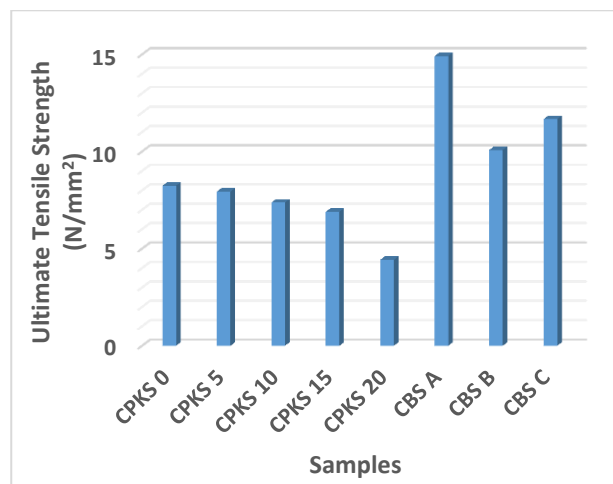


Fig. 10. Ultimate Tensile Strength (U.T.S.) for the Composite Materials.

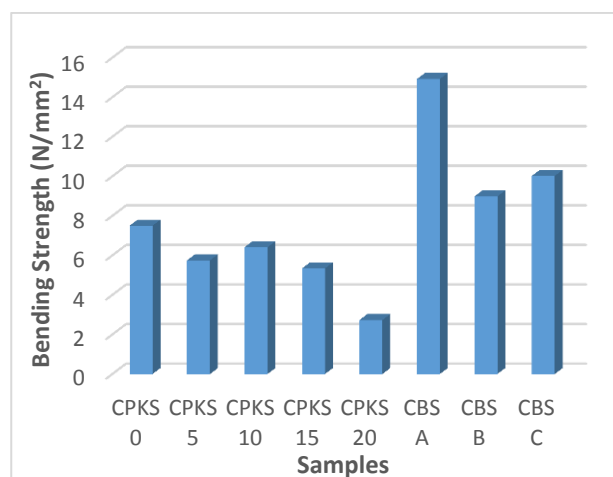


Fig. 11. Breaking Strength (B.S.) for the Composite Materials.

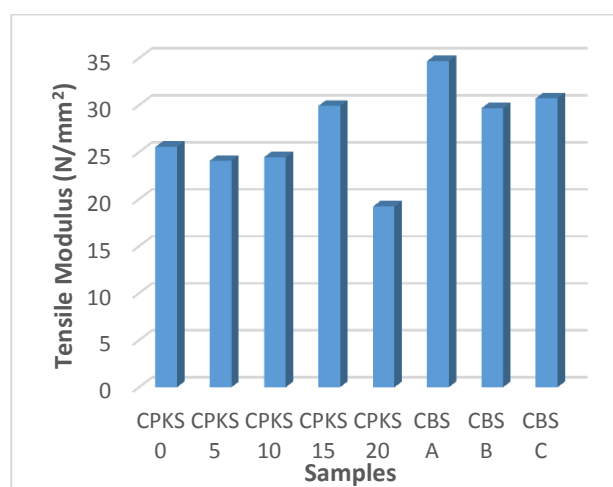


Fig. 12. Tensile Modulus (ϵ) for the Composite Materials.

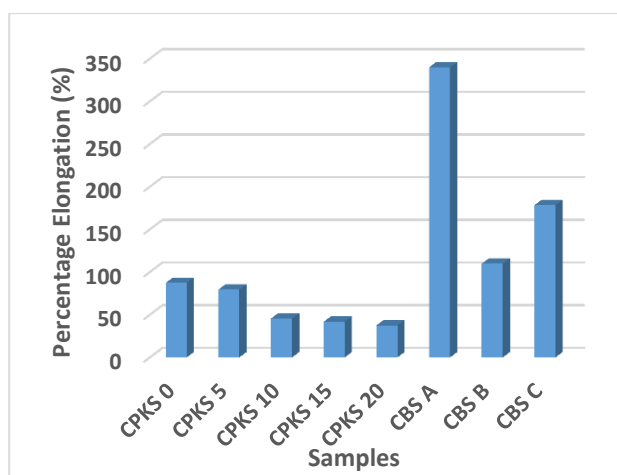


Fig. 13. Percentage Elongation (P.E.) for the Composite Materials.

The results of the tensile test carried out on the conventional bumper samples show that the material used in producing them have ultimate tensile strength (U.T.S) ranging from 10.08 to 14.92 N/mm². Their U.T.S. are relatively high compared to that of the composite materials who's highest is 7.94 N/mm² possessed by material with 5 wt% of CPKS.

Tensile strength of the composite materials decreases with increase weight fraction of CPKS particles in the matrix. It clearly indicates that addition of CPKS particles lowers the load bearing capacity of the composites. Introduction of reinforcements lowers the U.T.S. obtained from CPKS '5' sample from 8.24 N/mm² to 7.94 N/mm² up to 4.43 N/mm² possessed by CPKS '20'. This is 46.24 % reduction. The decrement in tensile strength is due to the poor surface area of particles in the matrix (see Figs. 7-9). The sizes of CPKS particles which is in micron (μm) range has low surface area leading to low interfacial bonding between the hydrophilic particles and hydrophobic matrix polymer. This led to decreased in the tensile strength as observed by [11] in their work. The graphical representation of the variations in the U.T.S. is shown on Fig. 10.

The Tensile Modulus of the composite material drops from 25.55 N/mm² to 24.08 N/mm² obtained in the material with 0 wt% CPKS sample, which now increase to a maximum value of 29.92 N/mm² obtained in the material with 15 wt% of CPKS, but dropped to 19.20 N/mm² on further introduction of reinforcement of CPKS particulate. This implies that the tensile modulus for the composite material increased to a peak value of

29.92 N/mm² in material with 15 wt% of CPKS then fell on further introduction of the particulate. The increase in tensile modulus with increasing CPKS particles loading is expected since the addition of particles increases the stiffness of the composites, which in turn decreases the elongation at break. The graphical representation of the variation in the tensile modulus for the composite material is shown on Fig. 12.

Also, introduction of reinforcement lowers the percentage elongation of the composite material from 87.29 % to 37.50 %, which is 49.79 % reduction. This can be attributed to the presence of two (2) Hard and brittle phases in the matrix. The variation in the percentage elongation for the composite material is shown on Fig. 13. This result agrees with that obtained by [12].

There was a special behaviour displayed by CPKS '10', which is its ability to work harden after it has plasticized. This occurs at about 30 % strain which might have contributed to the increase in its breaking load.

Finally, the tensile test results of the composite material, when compared to the properties obtained during the pre-analysis carried out on the matrix material before processing, show that there was improvement in its properties, which included increase in Tensile Modulus and decrease in percentage elongation. This was achieved by processing and introduction of reinforcement. The results obtained from the tensile test of the composite material are in agreement with those obtained by other researchers [12, 17-20],

Hardness Properties

The Hardness Number for the composite material were determined at room temperature and recorded in Table 4.

Table 4. Hardness Number for the Composite Material.

| Samples | Hardness Number (HN) (Shores) |
|---------|----------------------------------|
| CPKS 0 | 50 |
| CPKS 5 | 56 |
| CPKS 10 | 57 |
| CPKS 15 | 61 |
| CPKS 20 | 68 |
| CBS A | 69 |
| CBS B | 62 |
| CBS C | 64 |

Figure below shows the graphical representations of Hardness Number of the composite materials.

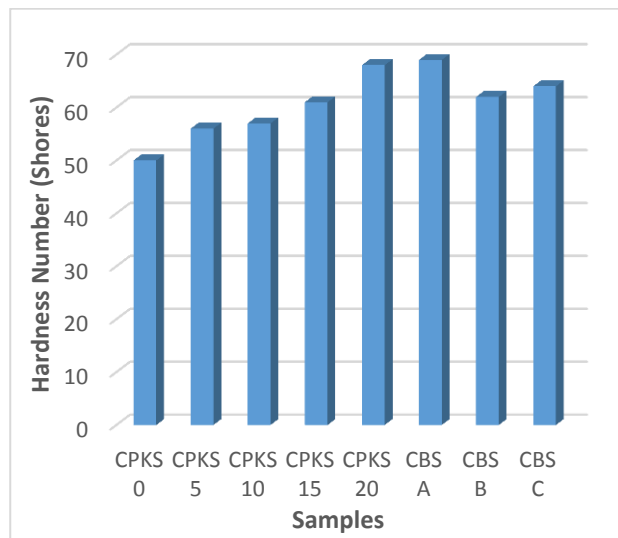


Fig. 14. Hardness Number for the Composite Materials.

The results obtained from the hardness test show that the hardness number of the composite material increases with increase in percentage composition of reinforcement (see Fig. 14). The hardness number increase from 50 Shores obtained CPKS '0' sample to 68 Shores from CPKS '20', which is 36 % increment. This is due to increase in the percentage of the hard and brittle phases of the ceramics body in the polymer matrix.

It was also noticed during testing that there was great variation in the hardness number of each composition when taken at different positions on the same sample as compared to that of conventional bumper sample, which was regular at different positions. This is associated with the distribution of the reinforcement in the matrix. This problem could be tackled by ensuring even distribution of reinforcement, using a systematic way of introducing the reinforcement into the matrix and allowing the compounding to take longer time for proper mixing.

The variation in the hardness number of the composite material also agrees with observations made by other researchers [11, 21-22].

Impact Energy

The impact energy absorbed before the material breaks are obtained from the scale on the testing

machine in pounds (lb). These were converted to Joule (J) then to Newton (N).The impact energy results are presented in Table 5.

Table 5. Impact energy for the Composite Material.

| Samples | Impact Load (lb) | Impact Energy (J) | Impact Energy (J/cm ²) | Impact Load (N) |
|---------|------------------|-------------------|------------------------------------|-----------------|
| CPKS 0 | 0.70 | 0.95 | 0.22 | 0.16 |
| CPKS 5 | 0.60 | 0.80 | 0.18 | 0.14 |
| CPKS 10 | 0.47 | 0.64 | 0.14 | 0.11 |
| CPKS 15 | 0.27 | 0.37 | 0.08 | 0.06 |
| CPKS 20 | 0.19 | 0.26 | 0.07 | 0.04 |
| CBS A | 0.80 | 1.08 | 0.26 | 0.17 |
| CBS B | 0.69 | 0.94 | 0.21 | 0.16 |
| CBS C | 0.73 | 0.99 | 0.22 | 0.17 |

Figure 15 shows the graphical representations of Impact strength of the composite materials.

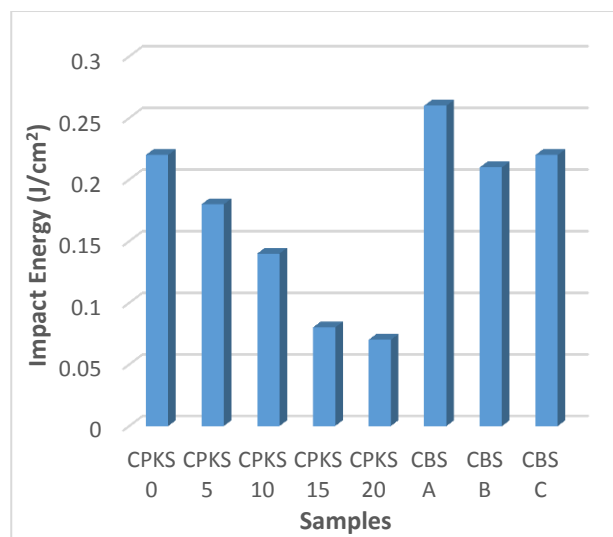


Fig. 15. Impact Strength for the Composite Materials.

The results of the impact test carried out on the composite material as recorded in Table 5 show that the impact energy of the material falls from 0.22 J/cm² obtained from CPKS '0' sample, as reinforcement was introduced into it, to 0.18 J/cm² obtained from CPKS '5' sample. This impact energy fell on further introduction of carbonized palm kernel shell to 0.07 J/cm² obtained in material with 20 wt% of CPKS.

This is mainly associated with reduction of elasticity of material due to particles addition and thereby reducing the deformability of matrix. An increase in concentration of CPKS particles reduces the ability of matrix to absorb energy and thereby reducing the toughness, therefore, impact strength decreases.

From Fig. 15, it is shown that the ability to resist impact force is higher in the unreinforced composite than those reinforced with CPKS, this is because the presence of the high carbon content in the CPKS has introduced some brittleness as increase in hardness leads to a decrease in impact strength (See Table 4). The reduction in impact energy and strain at failure with increasing CPKS loading might also be due to the decreased deformability of a rigid interface between the particles and matrix.

The developed composites have lower area under the stress-strain curves as compared to those of conventional bumper sample, which implies that they have poor toughness. This is because rigid ceramics body such as CPKS act as barriers against the mobility of dislocations. Therefore, by increasing the content of CPKS, the rate of work hardening increases and this would lead to a decrease in toughness values. The increase in hardness is related with the increasing amount of hard CPKS particles in the matrix. On the other hand, as can be suggested from the impact test, the elastic behaviour of the matrix proportionately varies with the addition of the CPKS particles. As the loading of CPKS increases, the ability of the composites to absorb impact energy decreases however, the results obtained are within the standard level for bio-composites [13].

These results implies that the composite material containing 5 wt% of iron filings and 5 wt% of CPKS will absorb up to 0.18 J/cm² stress at room temperature before it fails. This does not automatically recommend it as material composition for bumper production because its density is required to be considered alongside the impact energy in the recommendation.

During the test, it was observed that samples of conventional bumper, material with 0 wt% CPKS, material with 5 wt% of CPKS and that with 10 wt% of CPKS do not break after impact but bent while samples of material with 15 wt% of CPKS and 20 wt% of CPKS broke during the test. This is associated with the role played by the presence of two (2) hard brittle phases in the matrix and their inter-phase relationship.

Density of PMCs

The mass of a rectangular bar of each sample was measured while their volumes are calculate

using the standard formula; length x breath x thickness. Their densities are calculated by dividing their masses by their volumes. The densities are summarized in Table 6.

Table 6. Densities for the composite materials.

| Samples | Mass (g) | Volume (cm ³) | Density (g/cm ³) |
|---------|----------|---------------------------|------------------------------|
| CPKS 0 | 4.3 | 6.71 | 0.640 |
| CPKS 5 | 6.0 | 8.55 | 0.702 |
| CPKS 10 | 5.0 | 6.61 | 0.756 |
| CPKS 15 | 5.5 | 6.62 | 0.831 |
| CPKS 20 | 6.0 | 6.67 | 0.900 |
| CBS A | 3.0 | 2.63 | 1.140 |
| CBS B | 2.6 | 2.50 | 1.035 |
| CBS C | 2.7 | 2.44 | 1.091 |

Figure 16 shows the graphical representation of the densities of the composite materials.

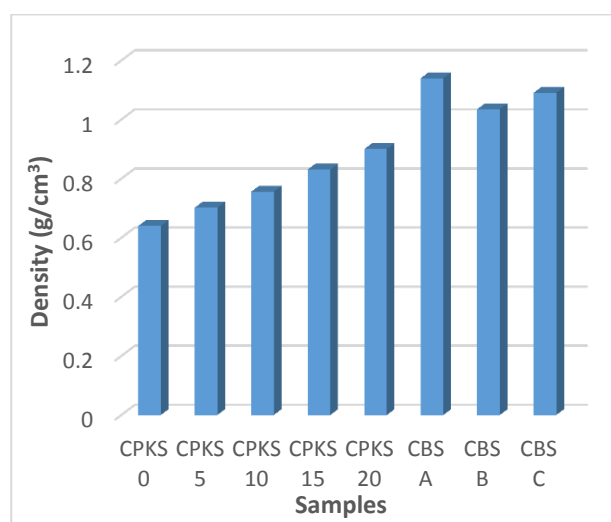


Fig. 16. Densities for the Composite Materials.

Table 6 shows the results obtained from the measurement of the composite material's density while Fig. 10 shows the variation with increase in percentage by weight of carbonized palm kernel shell as compared to the conventional bumper samples. The increment in the density of the composite material comes from the processing of the material, which include compounding and pressing. Pressing plays a major role in the improvement as it increase the compatibility of the material.

From the experimental results, the density of the composite material increase from 6.40 g/cm³ to 9.00 g/cm³, this is about 42.6 % increment. Their densities are low as compared to those of conventional bumper sample which varies from 1.035 to 1.14 g/cm³. This implies that any

composition selected for bumper production out of the composite material will save weight from the current overall weight of the car, these results agrees with earlier work carried out by other researcher [18].

Impact Energy – Density Ratio

This is the principal factor of consideration in choosing material for bumper fabrication. This indicates a material that is averagely light and withstands higher impact force. The compositions with the high Impact Energy – Density Ratio as shown on Table 7 and Fig. 17 are recommended for parts production.

Table 7. Impact Energy – Density Ratios for the composite materials.

| Samples | Impact Energy (J/cm ²) | Density (g/cm ³) | Impact Energy – Density ratio |
|---------|------------------------------------|------------------------------|-------------------------------|
| CPKS 0 | 0.22 | 0.640 | 0.34 |
| CPKS 5 | 0.18 | 0.702 | 0.26 |
| CPKS 10 | 0.14 | 0.756 | 0.19 |
| CPKS 15 | 0.08 | 0.831 | 0.10 |
| CPKS 20 | 0.07 | 0.900 | 0.08 |
| CBS A | 0.26 | 1.140 | 0.22 |
| CBS B | 0.21 | 1.035 | 0.20 |
| CBS C | 0.22 | 1.091 | 0.20 |

Figure 17 shows the graphical representation of the Impact Energy – density ratios of the composite materials.

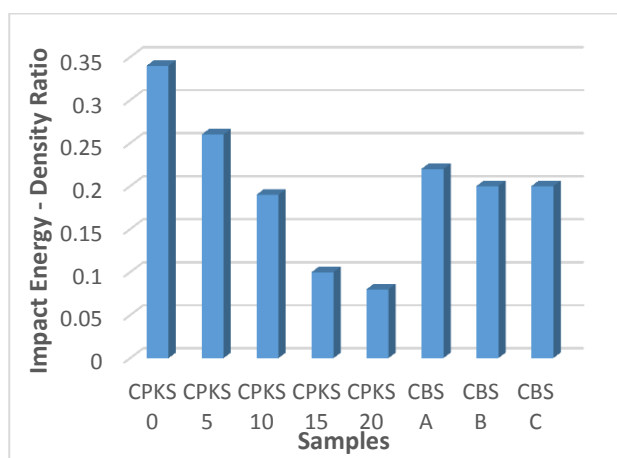


Figure 17. Impact Energy – Density Ratio for the Composite Materials.

The impact energy to density ratio was selected as a criterion for recommending material composition for bumper production because the functional requirement of a bumper is to absorb substantial level of impact load before failing. At

the same time, the density of the material should be considerably low so as not to increase the overall weight of the car.

The impact energy to density ratio was used to obtain a material that has high specific impact energy. Material with 5 wt% of CPKS was the least dense and has impact energy of 0.18 J/cm², so its ratio factor is 0.26, while material with 10 wt% of CPKS being little denser than the former, also absorbed an impact energy of 0.14 J/cm², making its ratio factor to be 0.19.

The results obtained show that the impact energy to density ratio for the conventional bumper samples were relatively low to that of the composite material. This is due to their high density ranging from 1.035 to 1.14 g/cm³ as compared to the highest obtained in the composite material, which is 9.00 g/cm³ and their low impact energy, as compared to those obtained in some of the composite material.

Two (2) compositions can be recommended for use in bumper production, which are materials with 5 wt% of CPKS and 10 wt% of CPKS, due to their high impact energy to density ratio.

4. CONCLUSION

This research work, among many has provided another way of converting commercial wastes, especially empty water sachets, which have turned into a national problem, into a useful material. After the whole tests and analyses, the following conclusions were drawn:

- The composite material was produced using compression moulding process.
- Most of the Mechanical Properties of the composite materials were reducing with increase in the percentage composition of CPKS which make them lower to those of CBS.
- Composite materials with 5 wt% of CPKS and 10 wt% of CPKS were recommended for use in the production of automobile bumper. This was based on their high impact energy to density ratio of 0.26 and 0.19 respectively, which is close to that of the standard, failure mode exhibited during testing (i.e. ductile failure) and their ability to work hardens after yielding during loading.

- The newly developed material is recommended for bumper production.

Acknowledgement

I want to appreciate the support of former occupant of the SHELL Professorial Chair, Mechanical Engineering Department, Ahmadu Bello University, Zaria, Nigeria.

REFERENCES

- [1] Use of Composite Material in Automotive Engineering, available at: <http://www.thinkengineering.com>, accessed: 07.09.2011.
- [2] E. Indino, 'Design and structural simulation of composites in transportation', in: *Proceedings of the Conference on the use of composite materials in vehicle design*, 28.06.2002, Genoa, Italy, Paper 2.
- [3] I.A. Samotu, M. Dauda, D.O. Obada and A.A. Alabi, 'Waste to wealth: A case study of empty water sachet conversion into composite material for automobile application', *Engineering*, vol. 11, no. 3, 199-208, 2014.
- [4] Palm Kernel Shell in the Manufacture of Automotive Brake Pad, available at: <http://www.rmrddtechnoexpo.com>, accessed: 30.10.2011.
- [5] Y. Aishat, 'Development of Fibre-reinforced Plastic for Automobile Application', *B. ENG thesis, Department of Chemical Engineering, Ahmadu Bello University, Zaria*, 1998.
- [6] S. Abdulwahab, 'Polyester Composite Development using Bone as Reinforcement', *B. ENG thesis, Department of Chemical Engineering, Ahmadu Bello University, Zaria*, 2002.
- [7] H. Salmah, A. Romisuhani and H. Akmal, 'Properties of low-density polyethylene/palm kernel shell composites: Effect of polyethylene co-acrylic acid', *Thermoplastic Composite Materials*, vol. 26, no. 1, pp. 3-15, 2013.
- [8] P.J. Herrera-Franco, A. Valadez-Gonzalez, 'A study of the mechanical properties of shortnatural-fiber reinforced composites', *Composites*, vol. 36, pp. 597-608, 2005.
- [9] R.M. Mizanur, A. Mubarak and B. Khan, 'Surface treatment of coir (*Cocosnucifera*) fibers and its influence on the fibersphysico-mechanical properties', *Composites Science and Technology*, vol. 67, pp. 2369-2376, 2007.
- [10] N. Mohamad, M. Andanastuti, M. J. Ghazali, D.H. Mohd, C.H. Azhari, 'The Effect of Filler on Epoxidised Natural Rubber-Alumina Nanoparticles Composites', *Scientific Research*, vol. 24, no. 4, pp. 538-547, 2008.
- [11] S.C. Mishra, N.B. Nayak and A. Satapathy, 'Investigation on Bio-waste Reinforced Epoxy Composites', *Metallurgical and Materials Engineering Department*, vol. 0, no. 0, pp. 1-5, 2009.
- [12] T.W. Clyne, 'Comprehensive Composite Materials', *Metal Matrix Composite*, vol. 3, pp. 1-8, 2000.
- [13] A.K. Mohanty, M. Misra and L.T. Drzal, 'Sustainable bio-composites from renewable resources: opportunity and challenges in the green materials world', *Polymer and Environment*, vol. 10, pp. 19-26, 2002.
- [14] L.A. Pothan, S. Thomas and Neelakantan, 'Short Banana Fiber Reinforced Polyester Composites: Mechanical, Failure and Aging Characteristics', *Reinforced Plastics and Composites*, vol. 16, no. 8, pp. 744-765, 1997.
- [15] H. Shangjin, S. Keyu, B. Jie, Z. Zengkun, L. Liang, D. Zongjie and Z. Baolong, 'Studies on the Properties of Epoxy Resins Modified with Chain-Extended areas', *Polymer*, vol. 42, pp. 9641-9647, 2001.
- [16] I.A. Madugu, M. Abdulwahab and V.S. Aigbodion, 'Effect of iron fillings on the properties and microstructure of cast fibre-polyester/iron fillings particulate composite', *J. Alloys and Compound*, vol. 476, no. 1-2, pp. 807-811, 2009.
- [17] S. Donne, M.R. Krishnadev and R. Bouchard, 'Metal and ceramic matrix mechanical behaviour', *The Minerals Metals and Materials Society*, pp. 243-251, 1990.
- [18] A. Sagail and G. Leisk, *Heat treatment optimization of Alumina/Aluminium Metal Matrix Composites using the Taguchi approach*, Scripta Metallurgica et Material, pp. 871-876, 1992.
- [19] R. Asthana, *Solidification processing of reinforced metals*, Transport Technology, pp. 67-80, 1998.
- [20] S. Yetgin, O. Cavdar and A. Cavdar, 'The effects of the fibre contents on the mechanical properties of the adobes', *Construction and Building Materials*, vol. 22, pp. 222-227, 2008.
- [21] J. P. Cottu, J. J. Coudere, B. Viguier and L. Bernard, 'Influence of SiC Reinforcement on Precipitation and Hardening of a Metal Matrix Composite', *Journal of Material Science*, vol. 27, no. 11, pp. 3068-3074, 1992.
- [22] M. Vogelsang, R.J. Arsenault and R.M. Fisher, 'An In-Situ HVEM Study of Dislocation Generation at Al/SiC Interfaces in Metal Matrix Composites', *Metall. Trans.*, vol. 17, Part A, pp. 379-389, 1986.